The Effect of Etchant Concentration on Surface Morphology

Of Porous GaP Produced By Laser-Induced Etching

Khalid M. Omar

School of Physics

University of Science of Malaysia

11800, Penang, Malaysia

E-mail: khalhadithi@yahoo.com

Zahid H. Khan

Department of Physics, Jamia Millia Islamia, 110025-New Delhi, India

R. K. Soni & S. C. Abbi

Department of Physics, Indian Institute of Technology, 110016-New Delhi, India

Abstract

Porous GaP have studied and fabricated by using an argon-ion laser beam of energy 2.41 eV was to recording the Raman spectra. The peak position shifts in Raman spectra was observed at 398 cm^{-1} after etching. The Raman line is broad and asymmetric in comparison to the Raman line for crystalline GaP of 402 cm^{-1}. The weak structure near 350 cm^{-1} is a forbidden TO phonon, which arises due to structural disorder in the material. The peak that appears near 378 cm^{-1} is attributed to a surface phonon mode. The surface phonon frequency depends on the nanocrystalline size, shape and dielectric constant of the surrounding medium. We have studied the surface morphology of porous layers obtained by LIE of n-type GaP (100) substrates by using a Scanning Electron Microscope (SEM). The morphology of porous GaP layers changes rapidly with laser power densities and irradiation times. As well as both the size and shape of the structure depend on the nature and concentration of etchant solution.

Keywords: RS, SEM, Porous, GaP, LIE.

1. Introduction

The room temperature Raman scattering studies of first-order mode in samples etched with different laser power densities and radiation times of the argon-ion laser. The Raman studies of the first-order mode in the CW laser etched samples and phonon confinement for one, two and three-dimensional confinement models have been described. The results are analyzed in the quantum confinement effects on the electronic structure of nanocrystals and also estimated the average size of the nanocrystals. Etching process, Raman scattering and photoluminescence of porous GaP is obtained.

Raman scattering has become an important technique for the characterization of semiconductor quantum structures. The Raman Effect is an inelastic scattering process where the sample absorbs one photon while simultaneously emitting another photon of a different frequency. The difference in the energy of the incident and scattering photon is characteristic of the lattice vibrational mode and contains important information about the semiconductor. Raman scattering is an effective tool and a suitable method and has been widely used to investigate vibrational and structural properties of nanocrystals. (Kanesmitsu, 1993, Liu, 1994 & Xia, 1995) Moreover, it is used to estimate the characteristic size of nanocrystallites via the phonon confinement. In a bulk semiconductor material, the phonon-photon interaction is limited to the Brillouin-zone center, but in the case of a finite size crystal, the presence of quantum-size nanostructures relaxes the associated selection rules so that the Raman peak depends upon nanostructure shape and size parameters. For example, the peak shape gives information about the microstructure in the complex matrix of the porous layer.

The Raman spectra for these materials were show, for the first time, to be sensitive to surface phonon modes of clean semiconductors. (Tütüncü, 1996) Two surface gap modes as well as three additional surface phonon modes have been observed in InP. The exact determination of the positions and line-widths of these microscopic gap modes opens a new field of application in studying surface bonding, anharmonicity effects and coupling to other excitations. (Hinrichs, 1994)

The confinement of electrons and holes in quantum wires of GaP in the porous layer was proposed as the origin for the blue and UV emission bands in porous GaP. For the quantum confinement structure in the porous layer, the blue and UV emission is expected to be much stronger than the orange emission from bulk GaP. (Meijerink, 1996) The optical properties of the porous GaP are different from the properties of the original single crystal. The modification of the properties of GaP could be due to an intensification of the electron-phonon interaction in the submicron to nanometer size structures of the porous layer. (Zoteev, 1996) Quantum confinement also affects the excitonic properties of indirect-gap material, which is responsible for inducing an indirect to direct conversion for the character of optical transition.

In n-GaP made porous by anodization etching, the photocurrent response within the porous layer indicates an increase in the optical path length in the porous layer. When the absorption length (penetration depth) $(1/\alpha)$ is larger than the thickness of the porous layer, significantly large electron-hole pairs are created in that region. (Erne', 1996)

2. Characterization of GaP

The laser–induced etching process is used to create GaP nanostructure. This photosynthesis method is proposed as an alternative technique for our studies, and was pioneered by (Noguchi, 1994) who used the visible –light irradiation of Si wafers immersed in an aqueous HF solution to obtain the pore formation. (Noguchi, 1993) This method offers a fundamental technique for the selective formation of optical devices. The electrochemical etching is a common technique to prepare the porous Si, porous GaP, and different other semiconductor materials. Recently, a more advantageous technique has been used to produce a porous material, that is, laser-induced etching. (Rasheed, 2001, Omar, 2001, Yamamoto, 2000 & Koker, 1999) These opto-electronic devices need strong luminescence intensity and a control of the peak position of luminescence over a range of wavelengths that depend on the size distribution of nanocrystallites. The etching was carried out at a laser power density of 12 W.cm^{-2} and 15 min irradiation time (IT). An argon-ion laser beam of energy 2.41 eV (λ = 514.5 nm) was used for recording the Raman spectra.

2.1 Laser-induced etching

Like porous silicon formation, in n-type Si, valence band holes are required at the surface of the sample and during the chemical reaction of silicon wafer initiated that the holes reach the wafer surface, thereby this wafer is known to be inert in aqueous HF acid. The porous GaP in n-type GaP, the valence band holes are also required for the dissolution reaction, (Gomez Rivas, 2002)

$$(GaP)_n + 6h^+ \rightarrow (GaP)_{n-1} + Ga(III) + P(III) \tag{1}$$

The charge transfer occurs at the semiconductor-electrolyte interface when a semiconductor is immersed in aqueous solution, which contains the electron acceptor species. The photo-generated holes are directly transferred to the electrolyte solution in the pores when the motion of electrons in the porous GaP, which has to be done by employing a modulated photocurrent.

The electrical current enhances the etching process in the wafer when this current flows from the backside through the electrolyte of the wafer to complete the electrical circuit. The schematic diagram of laser-induced etching process is shown as under Figure1.

It is desirable to construct the surface with different pore size distributions. The experimental conditions are very important to characterize the nature of nanocrystallites and distribution sizes during the LIE process; the morphological study images the surface and the size distribution of crystallites and it is thus an important study. We can prepare the porous materials by the laser–induced etching on different substrates.

3. The phonon confinement model

The phonon confinement model is used to evaluate the crystallite size from the frequency downshift and peak broadening of the Raman line. Among the several models proposed, (Brandt, 1992 & Prokes, 1992) the quantum confinement model (*QCM*) is based on the confinement of lattice vibrations in nanocrystallites, and the peak position and shape is directly related to the size of crystallites.

The phonon confinement model has been developed to explain the Raman spectra of microcrystalline materials and it is based upon the fact that, in an infinite crystal, only the phonon near the center of Brillouin-zone $(\vec{q} = o)$ contributes to the Raman spectrum because of momentum conversation between incident and scattered photon.

3.1 Three-dimensional confinement in porous GaP

The phonon confinement model was developed by (Richter, 1981) to explain the frequency shift and broadening of the Raman line in microcrystalline Si. The model has been used to explain Raman line shapes and to estimate microcrystallite sizes in samples of Si (Richter, 1981 & Campbell, 1986) and GaAs. (Tiong, 1984 & Brauustein, 1989) Phonons from the center of the Brillouin-zone $(\vec{q} = o)$ contribute to the Raman signal in crystalline materials. The

Raman line shape is constructed by assuming a Lorentzian line shape centered at ω(q), with the line width of the infinite crystalline material, and this is then weighted by the modified wave-vector of the phonon caused by the finite size effect. Therefore, I (ω) is a Lorentzian centered at ω(0) with a line width of Γ.

$$I(\omega) = \int \frac{|c(0,q)|^2}{[\omega - \omega(q)]^2 + \left(\Gamma/2\right)^2} d^3 q \tag{2}$$

where, $\omega(q)$ is the phonon-dispersion curve, Γ is the natural line width, and $q = 0$ for zone-center first-order Raman scattering.

The confining function that we have used is a Gaussian given by

$$|c(0,q)|^2 = \exp\left[\frac{-q^2(L_0)^2}{a^2 \cdot 4}\right] \tag{3}$$

with q in units of $2\pi/a$, where a is a lattice constant (5.45 $A°$ for GaP) and L is in units of a.

Therefore, the three–dimensional (3D) Brillouin–zone integration in equation 2, can be approximated with a one-dimensional integration in a Brillouin-zone using an appropriately averaged dispersion curve,

$$I(\omega, L) = \int_0^1 \frac{\exp\left[-q^2(L_0)^2 / a^2 \cdot 4\right] \cdot 2 \cdot \pi \cdot q}{[\omega - \omega(q)]^2 + \left(\Gamma/2\right)^2} dq \tag{4}$$

where, $\omega(q)$ is an approximated one-dimensional phonon dispersion curve,

$$\omega(q) = A + B \cos(\pi \cdot \frac{q}{2}) \tag{5}$$

where, A= 365.3 cm^{-1} and B= 37 cm^{-1}.

The values of ω and Γ are taken as 402 cm^{-1} and 3.3 cm^{-1} for crystalline GaP, and L_0 is the quantum confinement dimension.

The shape of this averaged curve is similar to that used in Si, diamond and GaAs phonon confinement calculations. This model is based on the optical phonons at the center of Brillouin-zone $(\overset{r}{q} = o)$, contributing to the first-order Raman at 402 cm^{-1} from the crystal GaP. The momentum conservation in nanocrystals is relaxed due to breakdown of translation symmetry and optical phonons are confined within the nanostructures and optical phonons with $(\overset{r}{q} \neq o)$ are allowed for that reason to contribute to the first-order Raman mode as in equation 4.

3.2 The crystallite size distribution in porous GaP

The choosing of the single value of L of crystallite size in equation 4, determines the peak position of Raman line from porous GaP. The confinement dimensions of nanocrystallites give the position of Raman line and have been used to match the Raman line-shape from porous Si. (Le Rendu, 2001) However, the observed broad Raman line shape is a consequence of the crystallite size distribution around a mean value L_0 as well as the confining geometry. The size distribution function that we have used is a Guassian:

$$\Phi(L) = \frac{1}{\sqrt{2 \cdot \pi}} \cdot \frac{1}{\sigma} \cdot \exp\left[\frac{-(L - L_0)}{2 \cdot \sigma^2}\right] \tag{6}$$

where, L_0 and σ are parameters, which are called the mean and standard deviation of the crystallite size distribution. In the present work, these are taken as fitting parameters. The Gaussian functions for the crystallite size distribution in the phonon confinement model have been used to convolute equation 4 with the Gaussian of equation 6 for the total Raman intensity:

$$I(\omega, L) = \int_{L_1}^{L_2} \Phi(L) \cdot I(\omega, L) dL \qquad (7)$$

The peak position for the Raman mode is determined by L_0, which is the value of L for which $\Phi(L)$ is maximum. L_1 & L_2 are the minimum and maximum contributing nanocrystallites sizes (1 & 10 nm). A change in the mean nanocrystallite size, L_0, leads to shift in Raman peak position and variations of L_1 & L_2 values lead to changes in the Raman line shape broadening without changing the peak position.

By using equation 7, results of a calculation for the Raman line shape of GaP nanocrystallites of uniform size, $L_0 = 6$ nm and same fitting parameters, is shown in Figure 2. The spectra have peak position 400 cm^{-1}.

The particles in 3D and 2D can move around the origin of the Coulomb potential without directly touching the origin. But in 1D, it is always moving through the origin because the spatial direction of motion is restricted to one dimension. The spatial phase volume around the origin is given as $4\pi r^2 dr$, $2\pi r dr$ and $2dr$ for 3D, 2D and 1D, respectively, where spherical, circular and linear shell regions from r to r + dr are considered. One and two-dimensional structures remain as interesting alternatives for integrated opto-electronics; only three-dimensional ones can provide full control of spontaneous emission in all space directions with the ultimate perspective of three-dimensional opto-electronic. Three-dimensional structures of the order of an optical wavelength have attracted a great deal of attention because of their potential use in various applications.

The first-order Raman line shape for one, two and three-dimensional confinement in GaP with the Gaussian distribution function and an identical mean nanocrystallite size $L_0 = 3$ nm and $\sigma = 5$ nm are shown in Figure 3.

The theoretical calculation of first-order Raman line can be show in figure 4 for the three-dimensional confinement of phonons incorporating the Gaussian size distribution for different nanocrystallite sizes by using equation 7.

3.3 Raman spectra of porous GaP

The Raman spectrum of porous GaP which prepared by laser-induced etching technique (LIE) is shown in Figure 5. The Raman peak position shifts to a lower frequency of 398 cm^{-1} after etching.

The Raman line is broad and asymmetric in comparison to the Raman line for crystalline GaP, which has a narrow and symmetric shape centered at 402 cm^{-1}. The SEM images show a lateral structure with thin pore walls consisting of spherical nanostructures.

The downward shift of the LO phonon frequency and an increase broadening is apparent. The theoretical fit to the experimental curve is obtained by using a three-dimensional quantum confinement model incorporating appropriate size distribution. A shift in the frequency of the surface mode (not shown here) depends on the state of the surface of the pores. The average size estimated from the fitting procedure is 3 nm. The broadening of Raman line is caused by the size distribution, which is dependent on etching parameters; we have observed two other weak Raman lines besides intense LO phonon line at 398 cm^{-1}.

The weak structure near 349 cm^{-1} is a forbidden TO phonon, which arises due to structural disorder in the material. The peak at 378 cm^{-1} is attributed to a surface phonon mode. The surface phonon frequency depends critically on the nanocrystalline size, shape and dielectric constant of the surrounding medium. We have calculated surface phonon frequency (ω_s) considering a shape using: (Hayashi, 1982)

$$\omega_s^2 / \omega_T^2 = \left[\varepsilon_0 + \varepsilon_m \left(1/L - 1\right)\right] / \left[\varepsilon_\infty + \varepsilon_m \left(1/L - 1\right)\right] \qquad (8)$$

where, ω_T is the frequency of the TO phonon,

$\varepsilon_0 = 11.01$, $\varepsilon_\infty = 9.09$ are the static and high frequency dielectric constant,

$\varepsilon_m = 1.00$, in the case of air surrounding, and

L is the depolarizing factor (0.3 for cylindrical shape, 1/3 for sphere and 0.4 for non-spherical particle shape).

The calculated value of surface phonon frequency in air for cylindrical shape is in good agreement with the observed value.

The effect of the particle shape should be taken into account to explain the observed shift of surface mode frequency with respect to the dielectric constant of the surrounding medium. (Sarua, 1999)

4. Surface morphology

Many semiconductor compounds have been investigated in the porous form. Pore formation has been reported for GaP in many electrolytes. (Belogrokhov, 1994, Tiginyanu, 1997& Zavaritskaya, 1998) A majority of this work has focused on the light emission process, blue and UV- luminescence from porous GaP. (Anedda, 1995 & Stevens-Kalceff, 2001) Through GaP has an indirect band gap structure similar to silicon, the pore structure and pore formation is significantly

different. Surface morphology of porous semiconductors, in general, is known to be very complicated and depend strongly on fabrication conditions. In this work, we study the surface morphology of porous layers obtained by laser-induced etching of n-type GaP (100) substrates. The morphology of porous gallium phosphide layers changes rapidly with laser power densities and irradiation times.

4.1 The effect of electrolyte concentration

4.1.1 The HF with Ethanol

Porous GaP layers have been prepared by laser-induced etching from n-GaP, (100) orientation having carrier concentration 3.7×10^{17} cm^{-3}. The GaP substrate was immersed in HF acid 40% diluted by ethanol 50% and irradiated by an argon-ion laser (λ=514.5 nm) under different irradiation times and with a fixed power density of 12 W.cm^{-2}. The etching process was carried out for 5, 10 and 15 min.

It can be seen from the SEM micrographs that the surface morphology and pore structure of the etched GaP samples are quite different from sample etched with concentrated HF electrolyte. Figure 6 (a) shows the morphology of porous GaP sample that was irradiated for 5 min. The pore morphology is random with no sign of any preferential etching. There are coarse features in the micrometer range and, on top of them, fine features with size in the range below 250 nm. It appears that the photochemical etching produces a bimodal effect in the crystal size distribution with coarse structure supporting the fine nanometer size structure. (Oskam, 1997, Ottow, 1996 & Schuurmans, 1999)

With an increase in the irradiation time, the pores grow selectively along a preferred crystallographic direction. On increasing the etching time to 10 min, Figure 6 (b), the pore structure is more oriented, while for 15 min irradiation time, Figure 6 (c), the orientation probably change from (100) to (111) direction, under same etching conditions. The structures are more uniform and the pore dimension is around 150-200 nm. The pore diameter is same throughout.

4.1.2 The HF without Ethanol

For the laser power density of 12 W.cm^{-2}, a well-defined wire like pore structure is formed even for 5 min. irradiation time due to the large density of hole supplied at the semiconductor-electrolyte interface. The long wires running parallel to (111) direction have varying sizes. Therefore, the regular structures have been synthesized for 100 nm pore dimension under these parameters as can be seen in Figure 7 (a). At longer irradiation time of 10 min., the pore structure has grown deeper with thinner pore walls. Some of the pore walls are 20-50 nm in dimension as shown in Figure 7 (b). Further increasing the irradiation time to 15 min. the pore propagates deep into the substrate and the pore walls become extremely thin, in the range of 10-50 nm as can be seen in Figure 7 (c), the large portion of the walls is also etched away and pore walls become shorter. At much higher laser power density the pore structure becomes disordered and a hole is created in the substrate.

5. Conclusion

The SEM micrographs revealed that the pores grow in the (111) direction along gallium or phosphorous planes. The chemical reaction of the hole with phosphorous is stronger than with gallium due to the high reactivity of phosphorous. A choice of suitable power density and irradiation time could be used to control both the size and shape of the structures. The technique of laser-induced etching was successfully adopted to synthesize GaP nanoparticles. Also, if the laser energy is tuned, the etched structure could be created shallow or deeper into the substrate due to the variation in the penetration depth of the laser light.

The process of laser-induced etching is initiated by first absorbing band–gap photons by the semiconducting electrode immersed in HF electrolyte. Electron-hole pairs are created in the semiconductor, which then separate to form the space charge layer on the semiconductor. In anisotropic etching, the crystallographic orientation significantly determines the density, dimensions and shapes of pores. The SEM images show a lateral structure with thin pore walls consisting of spherical nanostructures.

Surface morphology and porosity of the layers were found to be essentially independent of the electrolyte solution, increasing the concentration of the electrolyte solution mainly increases the PL peak energy due to the high rate of etching. The porosity increases slightly with the increasing concentration of the solution at same etching conditions.

Raman studies of nanocrystals provide information on the behavior of the fundamental optical and vibrational properties. Raman scattering is very sensitive to the lattice microstructure. A phonon confinement model is employed to explain the Raman shift of phonon modes of a nanocrystal and describes the size confinement effect on lattice vibration wave functions.

The Raman scattering spectra of porous GaP have a number of characteristic features. Both LO and TO phonons are always simultaneously present in the porous GaP spectra.

References

Anedda, A. Serpi, A. karavanskii, V. A. Tiginyanu, I. M. & Ichizli,V. M. (1995).   Time resolved blue and ultraviolet photoluminescence in porous GaP. *Appl. Phys. Lett,* 67, 3316

Belogrokhov, A. I. Karavanskii,V. A. Obraztsov, A. N. & Timoshenko, V. Yu. (1994). Intense photoluminescence in porous gallium phosphide. *JETP Letter*, 60, 274

Brauustein, G. Tuschel, D. Chen, S. & Lee, S. T. (1989). Raman scattering study of lattice disorder in 1-MeV Si-implanted GaAs. *J. Appl. Phys.,* 66, 3515

Brandt, M. S. Fuchs, H. D. Stutzmann, M. Weber, J. & Cardona, M. (1992). The origin of visible luminescence from "porous silicon": A new interpretation. *Solid State Commun,* 81, 307

Campbell, I. H. & Fauchet, P. M. (1986). The effects of microcrystal size and shape on the one phonon Raman spectra of crystalline semiconductors. *Solid State Commun*, 58, 739

Erne', B. H. Vanmaekelbergh, D. & Kelly, J. J. (1996). Morphology and Strongly Enhanced Photoresponse of GaP Electrodes Made Porous by Anodic Etching. *J. Electrochem. Soc.*, 143, 305

Gomez Rivas, J. Lagendijk, A. Tjerkstra, R. W. Vanmaekelbergh, D. & Kelly, J. J. (2002). Tunable photonic strength in porous GaP. *Appl. Phys*. Lett., 80, 4498

Hinrichs, K. Schierhorn, A. Haier, P. Esser, N. Richter, W. & Sahm, J. (1997). Surface Phonons of InP (110) Studied by Raman Spectroscopy. *Phys. Rev.* Lett, 79, 1094

Hayashi, S. & Kanamori, H. (1982). Raman scattering from the surface phonon mode in GaP microcrystals. *Phys. Rev.,* B 26, 7079

Koker, L. & Kolasinski, K.W. (1999). Observation and application of optical interference and diffraction effects in reflection. *J. Appl. Phys.,* 86, 1800

Kanesmitsu, Y. Uto, H. Masumuto, Y. Matsumoto T. Futagi, T. & Mimura, H. (1993). Microstructure and optical properties of free-standing porous silicon films: Size dependence of absorption spectra in Si nanometer-sized crystallites. *Phys. Rev.*, B 48, 2827

Le Rendu, P. Nguyen, T. P. Lakehal, M. Ip, J. Tiginyanu, I. M. Sarua, A. & Irmer, G. (2001). Poly (*p*-phenylene vinylene)/porous GaP composite materials. *Optical Materials*, 17, 175

Liu, X. N. Wu, X. W. Bao, X. M. & He, Y. L. (1994). Photoluminescence from nanocrystallites embedded in hydrogenated amorphous silicon films. *Appl. Phys*. Lett, 64, 220

Meijerink, M. Bol, A. A. & Kelly, J. J. (1996). The origin of blue and ultraviolet emission from porous GaP. *Appl. Phys*. Lett, 69, 2801

Noguchi, N. & Suemune, I. (1994). Selective formation of luminescent porous silicon by photosynthesis. J. *Appl. Phys*., 75, 4765

Noguchi, N. & Suemune, I. (1993). Luminescent porous silicon synthesized by visible light irradiation. *Appl. Phys*. Lett, 62, 1429

Omar, K. M. Soni, R. K. Rasheed, B. G. Abbi, S. C. & Khan, Z. H. (2001). Synthesis and Optical Properties of Porous GaP. Proc. "Physics of Semiconductor Devices", Indian Institute of Technology, *New Delhi, India,* Vol. 1, 248

Oskam, G. Natarajan, A. Searson, P. C. & Ross, F. M. (1997). The formation of porous GaAs in HF solutions. Appl. Surf. Sci., 119, 160

Ottow, S. Lehmann, V. & Foll, H. (1996). Processing of three-dimensional microstructures using macroporous n-type silicon. *J. Electrochem. Soc*., 143, 385

Prokes, S. M. Glembocki, O. J. Bermudez, V. M. Friedersdorf, L. E. & Searson, P. C. (1992). SiH$_x$ excitation: An alternate mechanism for porous Si photoluminescence. *Phys. Rev.*, B45, 13788

Rasheed, B. G. Mavi, H. S. Shukla,A. K. Abbi, S. C. & Jain, K. P. (2001). Surface reconstruction of silicon and polysilicon by Nd: YAG laser etching: SEM, Raman and PL studies. *Mat. Sci. & Eng.,* B 79, 71

Richter, H. Wang, Z. P. & Ley, L. (1981). The one phonon Raman spectrum in microcrystalline silicon. *Solid State Commun*, 39, 625

Sarua, A. Tiginyanu, I. M. Uraski, V. V. Irmer, G. Monecke, J. & Hartnagel, H. L. (1999). Charge carrier distribution in free-standing porous GaP membranes studied by Raman spectroscopy. *Solid State Commun,* 112, 581

Stevens-Kalceff, M. A. Tiginyanu, I. M. Langa, S. Foll, H. & Hartnagel, H. L. (2001). Correlation between morphology and cathodluminescence in porous GaP. *J. Appl. Phys.,* 89, 2560

Schuurmans, F. J. P. Vanmaekelbregh, D. Vande Lagenaat, J. & Lagendijk, A. (1999). Strongly Photonic Macroporous Gallium Phosphide Networks. *Science*, 284, 141

Tütüncü, H. M. & Srivastava, G. P. (1996). Surface phonons on InP (110) with the adiabatic bond-charge model. *Phys.*

Rev. B 53, 15675

Tiong, K. K. Amirtharaj, P. M. Pollack, F. H. & Aspnes, D. E. (1984). Effects of As[+] ion implantation on the Raman spectra of GaAs: "Spatial correlation" interpretation. *Appl. Phys. Lett*, 44, 122

Tiginyanu, I. M. Irmer, G. Monecke, J. & Hartnagel, H. L. (1997). Micro-Raman-Scattering study of surface-related phonon modes in porous GaP.   *Phys. Rev.*, B 55, 6739

Yamamoto, N. Sumiya, A. & Takai, H. (2000). Electroluminescence (EL) from photo-chemically etched silicon. *Mat. Sci. & Eng.* B, 69-70, 205

Xia, H. He, H. L. Wang, L. C. Zhang, W. Liu, X. N. Zhang, X. K. & Feng, D. (1995).   Phonon mode study of Si nanocrystals using micro-Raman spectroscopy. *J. Appl. Phys*. 78, 6705

Zoteev, A. V. Kashkarov, P. K. Obraztov, A. N. &   Timoshenko, V. Yu. (1996). Electrochemical formation and optical properties of porous gallium phosphide.   *Semiconductors*, 30, 775

Zavaritskaya, T. N. Kvit, A. V. Mel'nik, N. N. & Karavanskii, V. A. (1998). Amorphous, Glassy, and Porous Semiconductors. *Semiconductors*, 32, 213

Table 1. Fitting parameters of Figure 5, L_0 (mean value), L_1 and L_2 are minimal and maximum contributing nanocrystallite in equation 7.

Excitation photon energy (eV)	L_0 (nm)	L_1 (nm)	L_2 (nm)	σ (nm)	FWHM (cm^{-1})	Raman peak position (cm^{-1})
2.41	3	1	10	5	6.5	398

Table 2. Surface phonon frequency in air calculated by using equation 8.

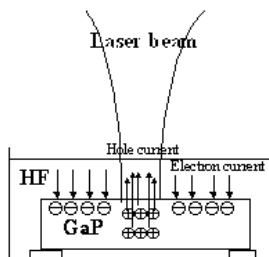| Surface phonon peak (cm^{-1})	TO phonon peak (cm^{-1})	Dielectric constant			Depolarizing Factor L
		ε_0	ε_∞	ε_m	
378	349	11.01	9.09	1.00	0.3

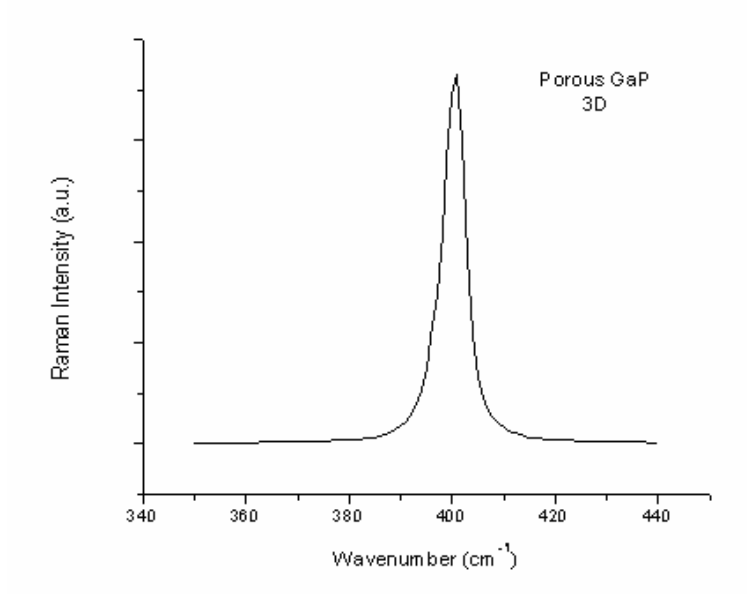Figure 1. Schematic diagram of Laser-induced etching process

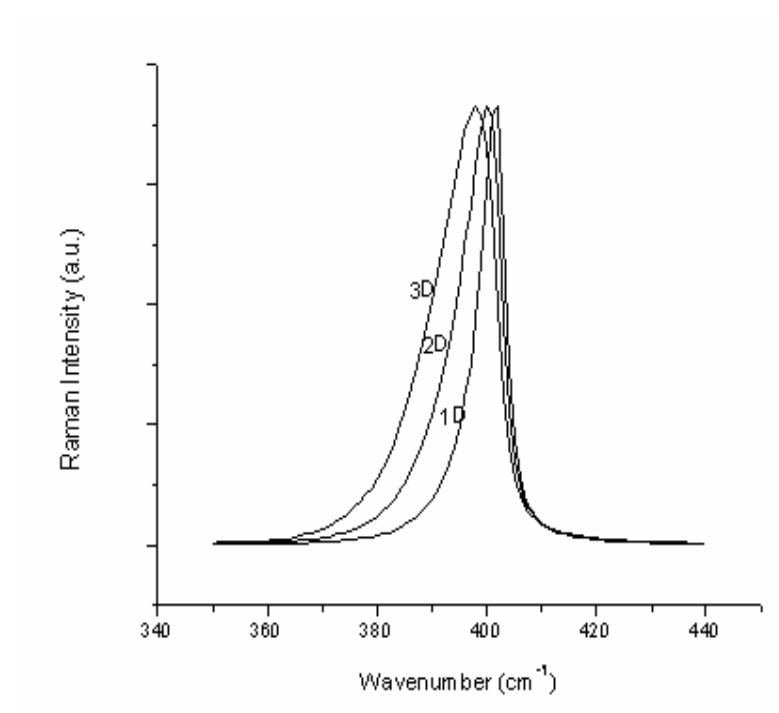Figure 2. Effect of the nanocrystallites size distribution.

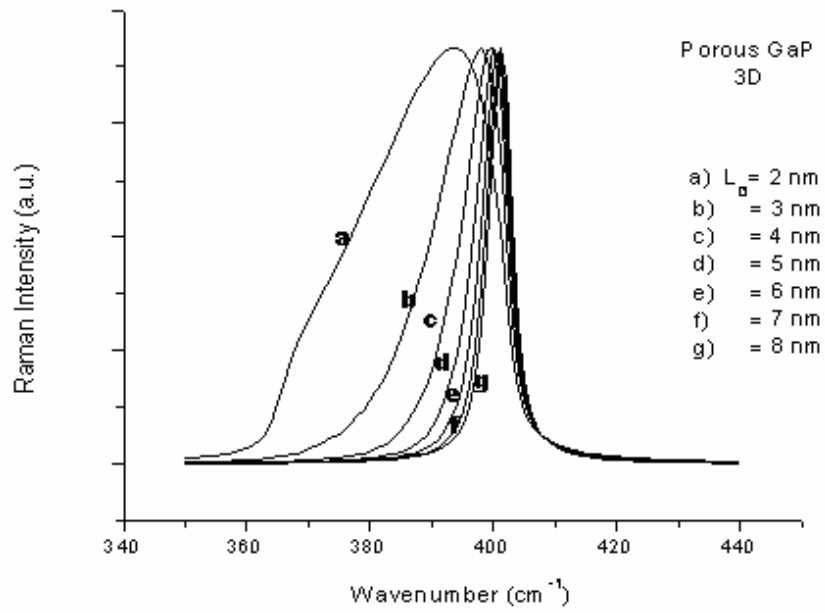Figure 3. One, two and three-dimensional confinement model for porous GaP

Figure 4. Size-dependent LO-phonon Raman line shape in GaP. Three-dimension
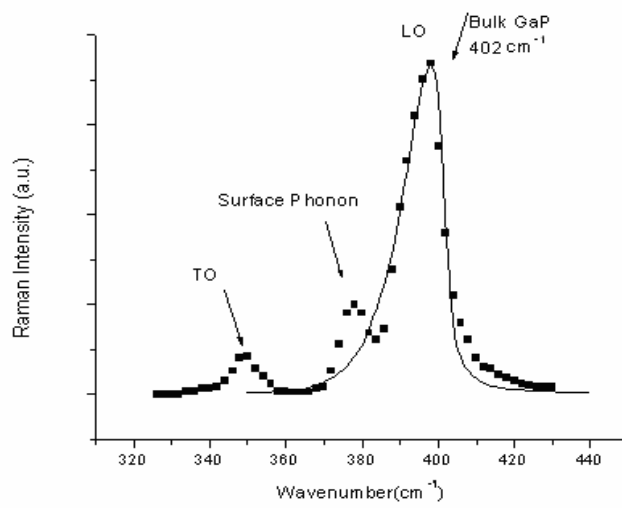Confinement geometry appropriate for sphere has been used.

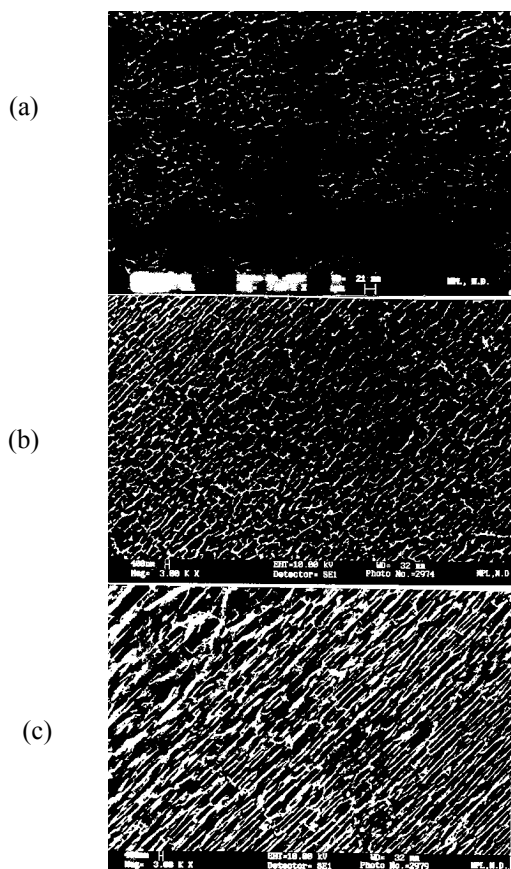Figure 5. Raman spectra of GaP nanostructure prepared by LIE

Figure 6. SEM images of porous GaP produced by LIE at 12 W.cm^{-2} for (a) 5 min, (b) 10 min, and (c) 15 min. with HF +Ethanol as electrolyte
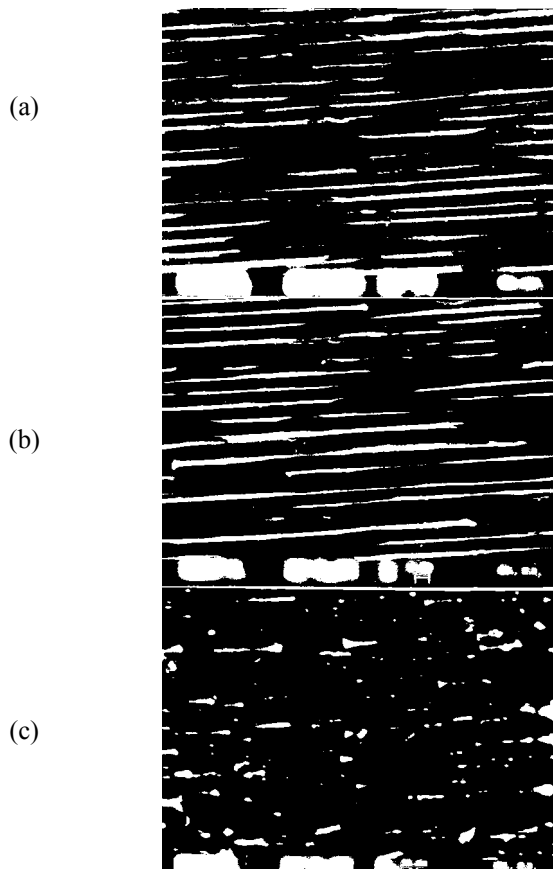

Figure 7. SEM images of porous GaP produced by LIE at 12 W.cm^{-2} for(a) 5 min, (b) 10 min, and (c) 15 min. with HF only